CPP

Contributions to Plasma Physics

www.cpp-journal.org

WILEY-VCH

REPRINT

Contrib. Plasma Phys. **49**, No. 4-5, 303 – 315 (2009) / **DOI** 10.1002/ctpp.200910028

Towards a Microscopic Theory of Particle Charging

F. X. Bronold[*1], **H. Fehske**[1], **H. Kersten**[2], and **H. Deutsch**[1]

[1] Institut für Physik, Ernst-Moritz-Arndt-Universität Greifswald, D-17489 Greifswald, Germany
[2] Institut für Experimentelle und Angewandte Physik, Christian-Albrechts-Universität zu Kiel, D-24098 Kiel, Germany

Received 23 March 2009, accepted 6 April 2009
Published online 2 June 2009

Key words Dusty or complex plasma, plasma-boundary interaction, surface states.
PACS 52.27.Lw, 52.40.Hf, 73.20.-r

We recently questioned the treatment of a dust particle as a perfect absorber for electrons and ions and proposed a surface model for the charge of a dust particle in a quiescent plasma which combines the microscopic physics at the grain boundary (sticking into and desorption from external surface states) with the macrophysics of the discharge (plasma collection fluxes). Within this model the charge and partial screening of the particle can be calculated without relying on the condition that the total electron collection flux balances on the grain surface the total ion collection flux. Grain charges obtained from our approach compared favorably with experimental data. The purpose of this paper is to describe our model in more detail, in particular, the hypotheses on which it is built, contrast it with the standard charging models based on flux balancing on the grain surface, and to analyze additional experimental data.

1 Introduction

Dust particles immersed in an ionized gas acquire charges whose signs and magnitudes strongly affect the properties of the host plasma as well as the properties of the ensemble of dust particles itself. The various crystalline and liquid phases of dust particles found in specifically designed laboratory experiments are perhaps the most impressive manifestations of this effect [1, 2]. That dust particles and host plasma are strongly coupled has been however known for a long time. Not only from astrophysical plasma environments [3, 4] but also from processing discharges, where the grains are of course not the intentional constituents studied for their own sake but contaminants which need to be controlled because they are detrimental to the overall performance of the discharge [5].

The charge of a dust particle is an important parameter for the quantitative description of dusty plasmas. It has thus been measured in a number of experiments [6–12]. Considering the dust particle as a floating electric probe, the interpretation of the experiments is based on two main assumptions: (i) The grain is a perfect absorber for electrons and ions, that is, every electron and ion hitting the surface of the grain is absorbed and (ii) the quasi-stationary charge of the dust particle is the one which balances on the grain surface the total electron collection flux with the total ion collection flux [13–19]. The charge enters here through the floating potential of the dust particle which, for a spherical particle, can be immediately translated into a charge. In most cases, however, the charges obtained from this approach are not in agreement with experimental data. Usually, the approximations for the fluxes are blamed for the disagreement [16, 18–23]. We suspect, however, that the flux balance condition, as it is currently used, is incomplete because it ignores important processes on the grain surface which also affect the grain charge.

First indications that this could be indeed the case came from a phenomenological analysis of experimental data based on rate equations for the electron and ion surface densities of a dust particle [24]. To provide a more realistic model for the grain surface, the rate equations contained electron and ion sticking probabilities, electron and ion desorption times, and a electron-ion recombination probability. With an appropriate choice of these parameters as well as the grain temperature the charges obtained from the quasi-stationarity of the surface

*Corresponding author: e-mail:bronold@physik.uni-greifswald.de

densities were in better agreement with experimental data then the ones deduced from the orbital motion limited flux balance condition.

In a semi-microscopic approach we subsequently pointed out that the charging of a dust particle can be interpreted as a physisorption process in the potential which builds up in the disturbed region around the grain [25]. The potential is the sum of a short-range polarization potential which enforces the electric boundary conditions on the grain surface and, as soon as the grain collected some charge, a long-range Coulomb potential. Realizing that the analogy to physisorption suggests, on a microscopic scale, a spatial separation of bound electrons and ions, we calculated the charge of the grain and its partial screening by balancing, on two different effective surfaces, the electron collection flux with the electron desorption flux and the ion collection flux with the ion desorption flux. The charge of the dust particle thereby obtained is then given by the number of electrons quasi-bound in the polarization-induced short-range part of the particle potential whereas its partial screening is given by the ions quasi-trapped in the long-range Coulomb part of the particle potential.

In this paper we discuss the surface model proposed in [25], in particular, the hypotheses on which it is built, in more detail and contrast the model with the standard approaches of calculating the particle charge from flux balancing on the grain surface. Thereby we identify certain issues which need to be resolved before a more refined microscopic theory of particle charging can be developed. Finally, to demonstrate that the surface model in its present form works we analyze further experimental data and show that the charges obtained from it are much better than the ones deduced from the standard approaches.

2 Elementary surface processes

The microphysics at the grain surface affecting the charge of the grain is schematically shown in the left panel of Fig 1. Electrons and ions are collected from the plasma with collection fluxes $j_{e,i}^{\rm coll} = s_{e,i} j_{e,i}^{\rm plasma}$, where $s_{e,i}$ are the sticking coefficients and $j_{e,i}^{\rm plasma}$ are the fluxes of plasma electrons and ions hitting the grain surface. Electrons and ions may thermally desorb from the grain surface with rates $\tau_{e,i}^{-1}$, where $\tau_{e,i}$ are the desorption times. They may also move along the surface with mobilities $\mu_{e,i}$, which in turn may affect the probability α_R with which ions recombine with electrons on the surface. All these processes occur in a thin layer whose thickness is at most a few microns, that is, on a scale where the standard kinetic description of the gas discharge based on the Boltzmann-Poisson system to which the flux balance condition belongs breaks down.

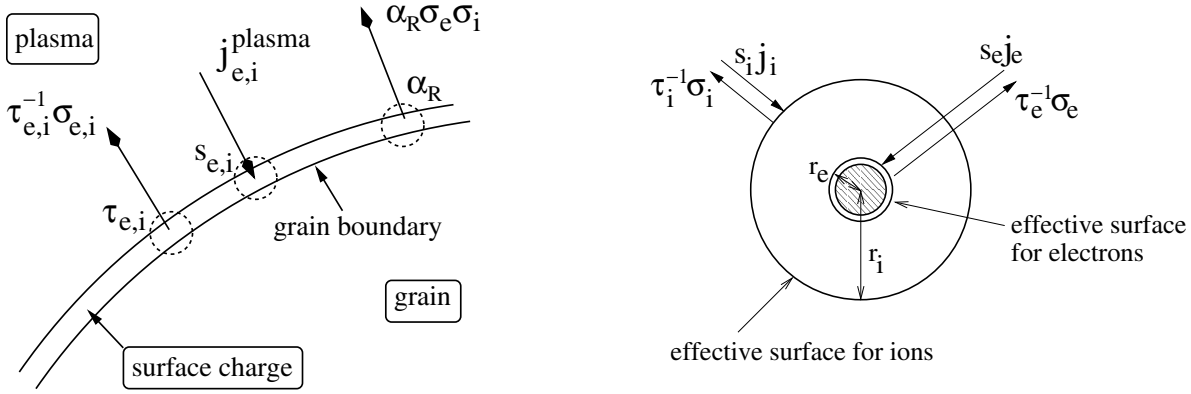

Fig. 1 Left panel: Generic illustration of elementary surface processes leading to the formation of surface charges at an inert plasma boundary where surface modifications other than charge accumulation do not occur. Right panel: Surface model proposed in [25] for the region around a dust particle with radius R. At quasi-stationarity, the surface charges $\sigma_{e,i}$ bound at $r_e \simeq R$ and $r_i \gtrsim r_e$, respectively, balance the collection fluxes $s_{e,i} j_{e,i}^{\rm plasma}$ with the respective desorption fluxes $\tau_{e,i}^{-1}\sigma_{e,i}$, where $s_{e,i}$ and $\tau_{e,i}$ denote, respectively, sticking coefficients and desorption times.

To put the surface model proposed in [25] into context and to identify the assumptions with respect to the surface properties which are usually made in the standard calculations of surface charges we cast the elementary surface processes into rate equations.

Specifically, we consider a spherical dust particle with radius R. The quasi-stationary charge of the grain is given by (we measure charge in units of $-e$)

$$Z_p = 4\pi R^2 \sigma_p = 4\pi R^2 \left[\sigma_e - \sigma_i\right] , \tag{1}$$

with electron and ion surface densities, $\sigma_{e,i}$, satisfying the quasi-stationary ($d\sigma_{e,i}/dt = 0$) rate equations [24],

$$0 \;=\; s_e j_e^{\rm plasma} - \tau_e^{-1}\sigma_e - \alpha_R \sigma_e \sigma_i \; , \tag{2}$$

$$0 \;=\; s_i j_i^{\rm plasma} - \tau_i^{-1}\sigma_i - \alpha_R \sigma_e \sigma_i \; . \tag{3}$$

where $j_{e,i}^{\rm plasma}$, $s_{e,i}$, $\tau_{e,i}$, and α_R have been introduced above. For simplicity we neglect diffusion along the surface.

In order to derive the standard criterion invoked to determine the quasi-stationary grain charge, we now assume, in contrast to what we do in our model [25] (see below), that both electrons and ions reach the surface of the grain. In that case, both Eq. (2) and Eq. (3) are flux balances on the grain surface. At quasi-stationarity, the grain is charged to the floating potential. In energy units $U = Z_p e^2/R$. Because the grain temperature $kT_p \ll U$ the ion desorption rate $\tau_i^{-1} \simeq 0$. Equation (3) reduces therefore to $\alpha_R \sigma_e \sigma_i = s_i j_i^{\rm plasma}$ which transforms Eq. (2) into $s_e j_e^{\rm plasma} = s_i j_i^{\rm plasma} + \tau_e^{-1}\sigma_p$ provided $\sigma_p \simeq \sigma_e$ which is usually the case. In the standard approach the grain surface is assumed to be a perfect absorber for electrons and ions. Thus, $s_i = s_e = 1$ and $\tau_e^{-1} = 0$. The quasi-stationary charge Z_p of the grain is then obtained from the condition

$$j_e^{\rm plasma}(Z_p) = j_i^{\rm plasma}(Z_p) \; , \tag{4}$$

where we explicitly indicated the dependence of the plasma fluxes on the grain charge.

Calculations of the grain charge differ primarily in the approximations made for the plasma fluxes $j_{e,i}^{\rm plasma}$. For the repelled species, usually collisionless electrons, the flux can be obtained from Poisson's equation and the collisionless Boltzmann equation, using trajectory tracing techniques based on Liouville's theorem and momentum and energy conservation [13, 14, 17]. The flux for the attracted species, usually collisional ions, is much harder to obtain. Unlike the electron flux, the ion flux depends not only on the field of the macroscopic body but also on scattering processes due to the surrounding plasma, which throughout we assume to be quiescent. For weak ion collisionalities the charge-exchange enhanced ion flux model proposed by Lampe and coworkers [20–22] is often used. Its validity has been however questioned by Tskhakaya and coworkers [26, 27]. We come back to Lampe and coworkers approach below when we discuss representative results of our model.

Irrespective of the approximations made for the plasma fluxes, the standard approaches of calculating surface charges are based on three assumptions about the surface physics:

(i) Ions and electrons reach the surface, even on the microscopic scale,
(ii) $s_e = s_i = 1$ or at least $s_e = s_i$, and
(iii) $\tau_e^{-1} = 0$ or at least $\tau_e^{-1}\sigma_e \ll s_i j_i^{\rm plasma} = \alpha_R \sigma_e \sigma_i$.

Hence, electrons and ions hitting the surface of the grain are assumed to be completely absorbed. For low-temperature gas discharges, where average electron energies $kT_e \simeq 10\ eV$, this cannot be the case, however. Permanent implantation of electrons with this energy is very unlikely. Instead, electrons impinging with a few eV on a surface are either reflected, inelastically scattered or, when the surface potential supports bound states, temporarily trapped in external surface states, with residence times depending on the inelastic coupling of the electrons to the elementary excitations of the surface and the bulk material. As far as ions approaching the dust particle are concerned they can gain at most the floating energy of a few eV. They are thus also not able to enter the grain and to get permanently stuck. [1]

Based on these considerations, the three assumptions concerning the grain surface made in the standard calculations of the grain charge seem to be rather unrealistic. We challenge therefore all three of them.

First, electrons and ions should be bound in external surface states. Because of differences in the potential energy, mass, and size we expect the spatial extension of the electron and ion bound states, and thus the distance

[1] We do not account for ion neutralization due to electron capture within the disturbed zone of the grain.

of electrons and ions from the grain surface, to be different. On the microscopic scale, electrons and ions should be spatially separated.

Second, $s_e = s_i$ is quite unlikely. Usually, the sticking coefficient of heavy particles is determined by the coupling to vibrational excitations of the surface and the bulk material [28, 29]. This coupling is very strong. Thus, if ions reach the surface, as it is conventionally assumed, they would efficiently dissipate energy. The sticking probability would be thus large, that is, close to unity. Light particles, like electrons, on the other hand, couple only weakly to surface and bulk vibrations. We would thus expect $s_e \ll s_i$. In principle the coupling to other elementary excitations of the grain (plasmons, electron-hole pairs, ...) can compensate for the lack of coupling to lattice vibrations but how efficient this coupling really is is not at all obvious. In a recent exploratory calculation we found, for instance, that the electron sticking coefficient at metallic boundaries arising from the coupling to internal electron-hole pairs is also extremely small, at least when the Coulomb interaction between an internal and an external electron is realistically screened [30].

Third, if ions and electrons are indeed spatially separated, the two rate equations (without the recombination term) should be in fact interpreted as flux balances on two different effective surfaces as shown in the right panel of Fig. 1. In that case, $\alpha_R \sigma_i \sigma_e \ll \sigma_{e,i}/\tau_{e,i}$ and the surface charge Z_p would be determined by balancing on the grain surface the electron desorption flux, $\tau_e^{-1}\sigma_e$, with the electron collection flux, $s_e j_e^{\rm plasma}$. The corresponding balance of ion fluxes, to be taken on an effective surface surrounding the grain, would then yield a partial screening charge Z_i. Within this scenario, we would thus obtain

$$Z_p = 4\pi r_e^2 \cdot (s\tau)_e \cdot j_e^{\rm plasma}(Z_p)\,, \tag{5}$$

$$Z_i = 4\pi r_i^2 \cdot (s\tau)_i \cdot j_i^{\rm plasma}\,, \tag{6}$$

with $r_e \simeq R$ and $r_i \gtrsim r_e$, which are the equations proposed in [25]. The sticking into and desorption from external surface states is here encoded in the products $(s\tau)_{e,i}$. For electrons the product depends only on material parameters but for ions it also depends on plasma parameters.

3 Surface states

The starting point of our surface model was a quantum mechanical investigation of the bound states of a negatively charged particle in a gas discharge. More specifically, we considered the static interaction between an electron (ion) with charge $-e$ ($+e$) and a spherical particle with radius R, dielectric constant ϵ, and charge $Q_p = -eZ_p$.

As mentioned before, the interaction potential contains a polarization-induced part, arising from the electric boundary conditions at the grain surface, and a Coulomb tail due to the particle's charge [31, 32]. For both terms we adopted the simplest approximations. The Coulomb part is then the potential of a point charge whose magnitude is the charge of the grain and the polarization part is the classical image potential. More sophisticated treatments taking, for instance, the finite velocity of the approaching electron (ion) and the nonlocality of the polarization potential at short distances into account are possible but not needed at this stage of the investigation.

Measuring distances from the grain surface in units of R and energies in units of U, the interaction energy at $x = r/R - 1 > x_b$, where x_b is a lower cut-off, below which the grain boundary cannot be described as a perfect surface anymore, reads

$$\begin{aligned} V_{e,i}(x) &= \pm\frac{1}{1+x} - \frac{\xi}{x(1+x)^2(2+x)} \\ &\simeq \begin{cases} 1-\xi/2x & \text{electron} \\ -1/(1+x) & \text{ion} \end{cases} \end{aligned} \tag{7}$$

with $\xi = (\epsilon-1)/2(\epsilon+1)Z_p$.

The second line in Eq. (7) is an approximation which describes the relevant parts of the potential very well and yet permits an analytical calculation of the surface states. In Fig. 2 we plot $V_{e,i}(x)$ for a melamine-formaldehyde (MF) particle ($\epsilon = 8$, $R = 4.7\ \mu m$, and $Z_p = 6800$) embedded in a helium discharge with plasma density $n_e = n_i = 0.62\times10^9\, cm^{-3}$, ion temperature $k_B T_i = 0.04\, eV$, and electron temperature $k_B T_e = 2.2\, eV$ [24,33]. From the electron energy distribution, $f_e(E)$, we see that the discharge contains enough electrons which can overcome the Coulomb barrier of the particle which is the floating energy U. These electrons may get bound in

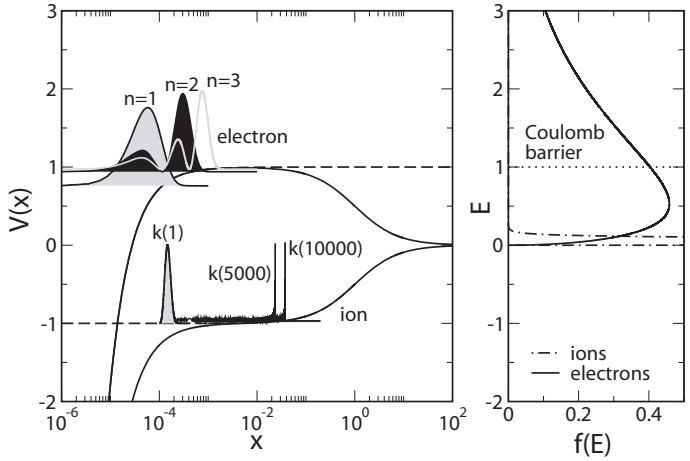

Fig. 2 Left panel: Potential energy for an electron (ion) in the field of a MF particle ($R = 4.7\ \mu m$, $Z = 6800$) [24, 33] and representative probability distributions, $|u(x)|^2$, shifted to the binding energy and maxima normalized to one. Dashed lines denote the potentials used in the Schrödinger equations. Note, the finite ion radius $\rho_i^{size} \simeq \mathring{A}$ forces the ion wavefunctions to vanish at $x \leq x_i^{size} \simeq 10^{-4}$. Right panel: Bulk energy distribution functions for the discharge hosting the particle [24, 33].

the polarization-induced short-range part of the potential, well described by the approximate expression, provided they can get rid of their kinetic energy. Ions, on the other hand, being cold (see $f_i(E)$ in Fig. 2) and having a finite radius $\rho_i^{size}/R = x_i^{size} \simeq 10^{-4}$, cannot explore the polarization potential at short distances [2]. For them, the long-range Coulomb tail is most relevant, which is again well described by the approximate expression.

Writing for the electron eigenvalue $\varepsilon^e = 1 - \alpha_e\xi/4k^2$ with $\alpha_e = (\epsilon - 1)R/4(\epsilon + 1)a_B$ and for the ion eigenvalue $\varepsilon^i = -\alpha_i/2k^2$ with $\alpha_i = m_i R Z_p/m_e a_B$, where a_B is the Bohr radius and m_e and m_i are the electron and ion mass, respectively, the radial Schrödinger equations for the approximate potentials read

$$\frac{d^2u^{e,i}}{dx^2} + \left[-\frac{\alpha_{e,i}^2}{k^2} + \tilde{V}_{e,i}(x) - \frac{l(l+1)}{(1+x)^2} \right] u^{e,i} = 0 \tag{8}$$

with $\tilde{V}_e(x) = 2\alpha_e/x$ and $\tilde{V}_i(x) = 2\alpha_i/(1+x)$. For bound states, the wavefunctions have to vanish for $x \to \infty$. The boundary condition at x_b depends on the potential for $x \leq x_b$, that is, on the surface barrier (which is different for electrons and ions). Matching the solutions for $x < x_b$ and $x > x_b$ at $x = x_b$ leads to a secular equation for k. For our purpose, it is sufficient to take the simplest model for the barrier: $\tilde{V}_{e,i}(x \leq x_b) = \infty$ with $x_b = 0$ for electrons and $x_b = x_i^{size}$ for ions.

The electron Schrödinger equation is then equivalent to the Schrödinger equation for the hydrogen atom and k is an integer n. Because (for bound electrons) $x \ll 1$ and $\alpha_e \gg 1$, the centrifugal term is negligible. Hence, we consider only states with $l = 0$. The eigenvalues are then $\varepsilon_n^e = 1 - \alpha_e\xi/4n^2$ and the wavefunctions read

$$u_{n,0}^e(x) \sim v_{n,0}(\bar{z}) = \bar{z}\exp(-\bar{z}/2)(-)^{n-1}(n-1)!L_{n-1}^{(1)}(\bar{z}) \tag{9}$$

with $\bar{z} = 2\alpha_e x/n$ and $L_n^{(1)}(\bar{z})$ associated Laguerre polynomials.

The probability densities $|u_{n,0}^e(x)|^2$ for the first three electron surface states are plotted in Fig. 2. As can be seen, they are very close to the surface. In physical units, the electron surface states are at most a few $\mathring{A}$ngstroms away from the grain boundary. At these distances, the spatial variation of $V_e(x)$ is comparable to the de-Broglie wavelength of electrons approaching the particle. More specifically, for $k_B T_e = 2.2\ eV$, $\lambda_e^{dB}/R \simeq |V_e/V_e'| \simeq 10^{-4}$. Hence, the trapping of electrons at the surface of the particle is a quantum-mechanical effect beyond the Boltzmann-Poisson description of the plasma-grain interaction.

The solutions of the ion Schrödinger equation are Whittaker functions, $u_{k,l}^i(x) = W_{k,l+1/2}(\bar{x})$ with $\bar{x} = 2\alpha_i(1+x)/k$ and k determined from $u_{k,l}^i(x_i^{size}) = 0$. However, since $\alpha_i \gg 1$ and $k \gg 1$, it is very hard to work

[2] We treat the ion as a structureless rigid sphere.

directly with $W_{k,l+1/2}(\bar{x})$. It is easier to use the method of comparison equations [34] and to construct uniform approximations for $u^i_{k,l}(x)$ with the radial Schrödinger equation for the hydrogen atom as a comparison equation. The method can be applied for any l. Here we give only the result for $l = 0$:

$$u^i_{k,0}(x) \sim v_{n,0}(\bar{z})/\sqrt{dz/dx} \tag{10}$$

with $v_{n,0}(\bar{z})$ defined in Eq. (9) and $\bar{z} = 2\alpha_i z(x)/n$. The mappings $z(x)$ and $k(n)$ can be constructed from the phase-integrals of the two ion Schrödinger equations [34].

In Fig. 2 we show $|u^i_{k,0}(x)|^2$ for $k(1)$, $k(5000)$ and $k(10000)$. Note, even the $k(10000)$ state is basically at the bottom of the potential. This is a consequence of $\alpha_i \gg 1$ which leads to a continuum of bound states below the ion ionization threshold at $\varepsilon = 0$. We also note that $|u^i_{k(n),0}(x)|^2$ peaks for $n \gg 1$ just below the turning point. Hence, except for the lowest ion surface states, which we expect to be of little importance, ions are essentially trapped in classical orbits deep in the disturbed region of the grain. This will be also the case for $l > 0$. That ions behave classically is not unexpected because for $k_B T_i = 0.04\ eV$ their de-Broglie wavelength is much smaller then the scale on which the potential varies for $x > 10^{-3}$: $\lambda^{dB}_i/R \simeq 10^{-5} \ll |V_i/V_i'| \simeq 1$. Thus, the interaction between ions and the dust particle is classical and can be analyzed with Boltzmann-Poisson equations.

Nevertheless it is also possible to describe this interaction quantum-mechanically. We anticipate even a quantum-mechanical approach, based on the method of comparison equations, which is an asymptotic technique well suited for the semiclassical domain we are interested in, to be rather useful in this respect. In fact, many years ago a wave-mechanical description of the collisionless ion dynamics around electric probes has been pursued by Liu [35] but he found no followers.

4 Charging model

Using the results of the previous section, a model for the grain charge taking surface states into account can be constructed as follows. Within the disturbed region of the particle, the density of free electrons (ions) is much smaller than the density of bound electrons (ions). In that region, the quasi-stationary charge (again in units of $-e$) is thus approximately given by

$$Z(x) = 4\pi R^3 \int_{x_b}^{x} dx' \big(1 + x'\big)^2 \Big[n^b_e(x') - n^b_i(x') \Big] \tag{11}$$

with $x < \lambda^D_i = \sqrt{kT_i/4\pi e^2 n_i}$, the ion Debye length, which we take as an upper cut-off, and $n^b_{e,i}$ the density of bound electrons and ions. For the plasma parameters used in Fig. 2, $\lambda^D_i \simeq 60\mu m$. The results for the surface states presented above suggest to express the density of bound electrons by an electron surface density:

$$n^b_e(x) \simeq \sigma_e \delta(x - x_e)/R \tag{12}$$

with $x_e \simeq x_b \simeq 0$ and σ_e the quasi-stationary solution of Eq. (2) without the recombination term. Equation (2) is thus still a rate equation on the grain surface. We will argue below that once the grain has collected some negative charge, not necessarily the quasi-stationary one, there is a critical ion orbit at $x_i \sim 1 - 10 \gg x_e$ which prevents ions from hitting the particle surface. Thus, the particle charge obtained from Eq. (11) is simply $Z_p \equiv Z(x_e < x < x_i)$. Inserting Eq. (12) into Eq. (11) and integrating up to x with $x_e < x < x_i$ leads to Eq. (5), the expression for the particle charge deduced from the rate equations (2) and (3) under the assumption that ions do not reach the grain surface on the microscopic scale.

For an electron to get stuck at (to desorb from) a surface it has to loose (gain) energy at (from) the surface [28]. This can only occur through inelastic scattering with the elementary excitations of the grain schematically shown in the left panel of Fig. 3. To calculate the product $(s\tau)_e$ requires therefore a microscopic model for the electron-grain interaction. First steps in this direction were taken in [30].

In Ref. [25] we invoked however the phenomenology of reaction rate theory to approximate $(s\tau)_e$. Specifically, we assumed that electrons with rather low and rather high energies are, respectively, reflected by the Coulomb and surface barrier of the particle and that sticking (desorption) primarily affects electrons with energies slightly above U. After overcoming the Coulomb barrier this group of electrons is almost in equilibrium

with the surface electrons. We can thus apply the Lennard-Jones-Devonshire formula [28, 36] to obtain,

$$(s\tau)_e = \frac{h}{k_B T_p} \exp\left[\frac{E_e^d}{k_B T_p}\right] , \tag{13}$$

where h is Planck's constant, T_p is the grain temperature, and E_e^d is the electron desorption energy, that is, the binding energy of the surface state from which desorption most likely occurs. The great virtue of this equation is that it relates a combination of kinetic coefficients, which depend on the details of the inelastic (dynamic) interaction, to an energy, which can be deduced from the static interaction alone. Kinetic considerations are thus reduced to a minimum. They are only required to identify the relevant temperature and the state from which desorption most probably occurs.

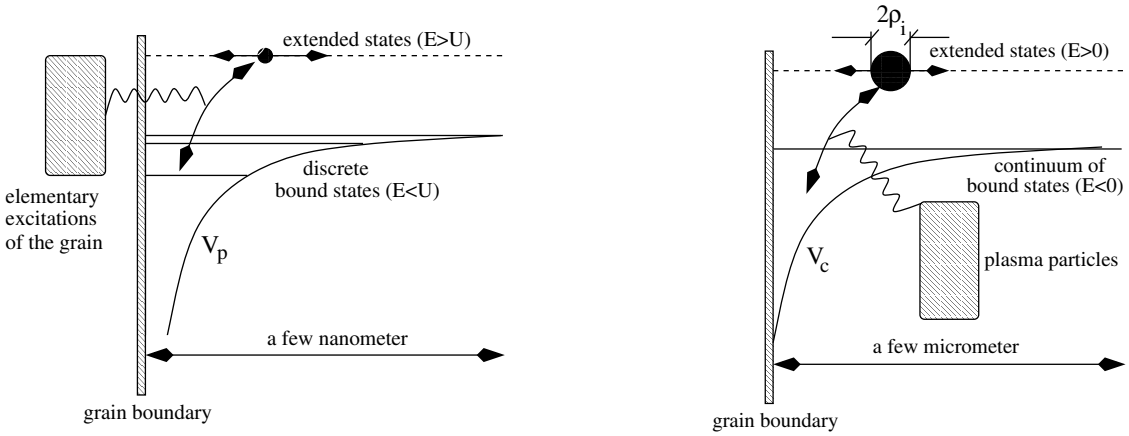

Fig. 3 Left panel: Schematic illustration of electron energy relaxation at the grain boundary. The electron looses (gains) energy due to creation (annihilation) of elementary excitations of the grain. Due to these processes it may get trapped in (escape from) the discrete bound states of the short-range polarization potential. Right panel: Schematic illustration of ion energy relaxation in the vicinity of the grain surface. The ion looses (gains) energy due to collisions with other plasma particles (electrons, ions, neutrals). It is due to these processes that an ion may get trapped in (escape from) the continuum of bound states of the long-range Coulomb potential.

Equation (5) is a self-consistency equation for Z_p. Combined with Eq. (13), and approximating the electron plasma flux $j_e^{\rm plasma}$ by the orbital motion limited flux,

$$j_e^{\rm OML} = n_e \sqrt{\frac{k_B T_e}{2\pi m_e}} \exp\left[\frac{-Z_p e^2}{R k_B T_e}\right] , \tag{14}$$

which is reasonable, because, on the plasma scale, electrons are repelled from the grain surface, the grain charge is given by

$$Z_p = 4\pi R^2 \frac{h}{k_B T_p} \exp\left[\frac{E_e^d}{k_B T_p}\right] j_e^{\rm OML}(Z_p) . \tag{15}$$

Thus, in addition to the plasma parameters n_e and T_e, the charge depends on the surface parameters T_p and E_e^d.

Without a microscopic theory for the inelastic electron-grain interaction, a plausible estimate for E_e^d has to be found from physical considerations alone. Since by necessity the electron comes very close to the grain surface it will strongly couple to elementary excitations of the grain (see Fig 2 and the left panel of Fig. 3). Depending on the material these may be bulk or surface phonons, bulk or surface plasmons, or internal electron-hole pairs. For any realistic surface barrier, where the electron wavefunction leaks into the solid, the electron will thus quickly relax to the lowest surface bound state [3]. The $n = 1$ state for the infinitely high barrier is an approximation to that state. Thus, it is reasonable to expect

$$E_e^d \simeq (1 - \varepsilon_1^e)U = \frac{R_0}{16}\left(\frac{\epsilon - 1}{\epsilon + 1}\right)^2 , \tag{16}$$

[3] The microscopic model for electron energy relaxation at metallic boundaries employed in [30] works also for an infinitely high barrier.

where ε_1^e is the lowest eigenvalue of the electronic Schrödinger equation. For an MF particle with $\epsilon = 8$ this leads to $E_e^d \simeq 0.5eV$. The particle temperature cannot be determined in a simple way. It depends on the balance of heating and cooling fluxes to-and-fro the particle and thus on additional surface parameters [37]. We use T_p therefore as an adjustable parameter. To reproduce, for instance, with Eq. (15) the charge of the particle in Fig. 2, $T_p = 395\ K$ implying $(s\tau)_e \simeq 10^{-6}\ s$.

Equation (15) depends on the assumption that once the particle is negatively charged ions are trapped far away from the grain surface. Indeed, treating trapping of ions in the field of the grain as a physisorption process suggests this assumption, which is perhaps counter-intuitive. Provided the ion remains intact on its way towards the grain surface (no ion neutralization in the disturbed zone of the grain due to electron capture) it gets bound to the grain only when it looses energy. Because of its low energy and the long-range attractive ion-grain interaction, the ion will be initially bound very close to the ion ionization threshold (see Fig. 2). The coupling to the elementary excitations of the grain is thus negligible and only collisions with other plasma particles are able to push the ion from an extended state with positive energy to a bound state with negative energy and then from a given bound state to a lower one (see the illustration in the right panel of Fig. 3). Since the interaction is classical, collisions, for instance, charge-exchange scattering between ions and atoms, act like a random force. Ion energy relaxation can thus be envisaged as a destabilization of orbits. This is in accordance to what Lampe and coworkers assume [20–22]. In contrast to them, however, we [25] expect orbits whose spatial extension is smaller than the scattering length to be stable because the collision probability during one revolution becomes vanishingly small. For a circular orbit, a rough estimate for the critical radius is $r_i = R(1 + x_i) = (2\pi\sigma_{\rm cx} n_g)^{-1}$ which leads to $x_i \simeq 5 \gg x_e \simeq 0$ when we use the parameters of the helium discharge of Fig. 2 and $\sigma_{\rm cx} = 0.32 \times 10^{-14}\ cm^2$ which is the measured cross section at $0.3\ eV$ [38, 39].

Indeed, Lampe and coworkers approach [20–22] shows a pile-up of trapped ions in a shell of a few μm radius enclosing the grain. They would however not expect a relaxation bottleneck. This point can be only clarified with a detailed investigation of the ion dynamics and kinetics in the disturbed region of the grain taking the complete kinematics of charge-exchange collisions encoded in the differential collision cross section and the centrifugal barriers separating bound from unbound ion motion into account. In fact, Lampe and coworkers neglect the momentum transfer during a charge-exchange collision as well as the barriers. Tskhakaya and coworkers [26, 27] on the other hand pointed out that the latter could severely overestimate the collision-enhanced ion flux. In reality, this flux, they claim, is much smaller than the one obtained by Lampe and coworkers. If this is indeed the case, the charges obtained from the collision-enhanced ion flux model would be much closer to the orbital-motion limited ones and thus far away from the experimentally measured charges (see next section).

Table 1 Plasma parameters [24, 33] used to obtain the results plotted in Fig. 4.

$P[W]$	$p[Pa]$	$n_e, n_i[10^9 cm^{-3}]$	$kT_e[eV]$	$kT_i[eV]$
5	102	0.33	1.5	0.030
12	102	0.62	2.2	0.040
20	102	0.9	1.7	0.035
30	102	1.2	1.28	0.036
40	102	1.5	1.2	0.038
50	102	1.4	1.0	0.039
60	102	1.6	0.8	0.040
12	30	0.26	2.2	0.030
12	40	0.4	2.2	0.030
12	60	0.48	2.2	0.030
12	80	0.52	2.2	0.036
12	102	0.62	2.2	0.040
12	120	0.8	2.2	0.040

In [25] we pushed the assumption of a critical ion orbit to its limit and approximated the density n_i^b of ions accumulating in the disturbed region of the grain, and being responsible for the partial screening of the grain charge, by a surface density σ_i which balances at x_i the ion charging flux with the ion desorption flux (see right panel of Fig. 1). Mathematically, this gives rise to a rate equation similar to (3), but without the recombination

term and interpreted as a rate equation at $r = r_i$. At quasi-stationarity, the ion surface density is thus $\sigma_i = (s\tau)_i j_i$. Although Eq. (13) assumes elementary excitations of the grain to be responsible for sticking and desorption we expect a similar expression (with E_e^d, T_p replaced by E_i^d, T_g) to control the density of trapped ions. Equation (11) leads then to $Z(x_i < x < \lambda_i^D) = Z_p - Z_i$ with

$$Z_i = 4\pi R^2 (1 + x_i)^2 \frac{h}{k_B T_g} \exp\left[\frac{E_i^d(Z_p)}{k_B T_g}\right] j_i^B \tag{17}$$

the number of trapped ions where we assumed that the critical ion orbit, which is near the sheath-plasma boundary, is fed by the Bohm ion flux $j_i^B = 0.6 n_i \sqrt{k_B T_e / m_i}$.

The ion desorption energy is the negative of the binding energy of the critical orbit,

$$E_i^d(Z_p) = -V_i(x_i) U = 4\pi \sigma_{\rm cx} a_B n_g Z_p R_0 \,, \tag{18}$$

and depends strongly on Z_p and x_i. For the situation shown in Fig. 2 we obtained, for instance, using $T_g = T_p = 395\ K$, the particle temperature which reproduces $Z_p = 6800$, $E_i^d \simeq 0.37\ eV$ and $(s\tau)_i \simeq 0.6 \times 10^{-8}\ s$. The ion screening charge is then $Z_i \simeq 148 \ll Z_p$ which is the order of magnitude expected from molecular dynamics simulations [40]. Thus, even when the particle charge is defined by $Z(x_i < x < \lambda_i^D)$ it is basically given by Z_p.

5 Results

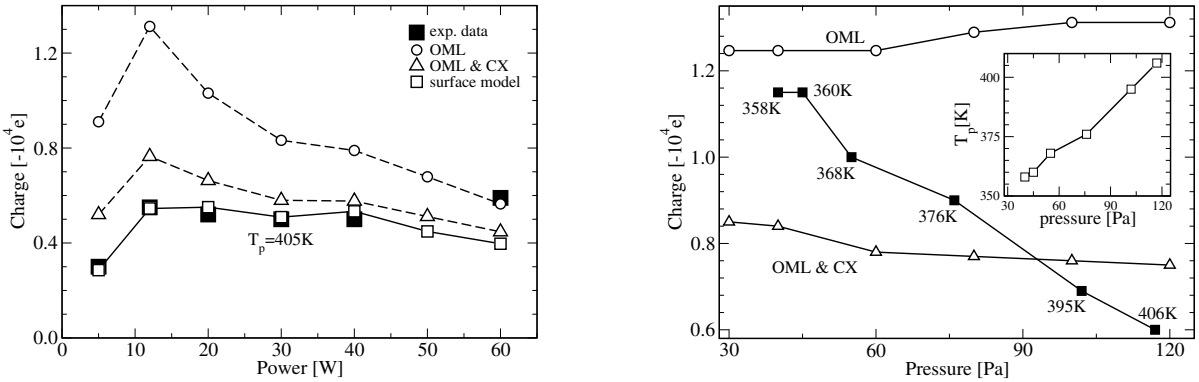

Fig. 4 Left and right panel show, respectively, the power and pressure dependence of the charge of a MF particle ($R = 4.7\ \mu m$) in the helium discharge of Ref. [33]. The particle temperatures reproducing the experimental data (filled squares) are indicated and the charges obtained from $j_e^{\rm OML} = j_i^{\rm OML}$ (OML) and $j_e^{\rm OML} = j_i^{\rm OML} + j_i^{\rm CX}$ (OML & CX) with $\sigma_{\rm cx} = 0.3 \times 10^{-14} cm^2$ [38,39], which is the measured cross section at $0.3\ eV$, are also shown. The predicted increase of the particle temperature with pressure is plotted in the inset of the right panel.

We now use Eq. (15) to calculate for various experimental set-ups the charge of a dust particle. In all cases the plasma parameters are known. The only free parameter is thus the particle temperature. Although there exist optical methods to measure the temperature of dust particles [41] they have not yet been used in conjunction with charge measurements. In view of the importance of the particle temperature for the surface model, we hope that in the near future an experimental group can be found to perform such measurements.

In addition to the results obtained from the surface model we also plot charges deduced from balancing the orbital motion limited electron flux $j_e^{\rm OML}$ given in Eq. (14) with, respectively, the orbital motion limited ion flux,

$$j_i^{\rm OML} = n_i \sqrt{\frac{k_B T_i}{2\pi m_i}} \left[1 + \frac{Z_p e^2}{R k_B T_i}\right] , \tag{19}$$

and the collision-enhanced ion flux (see [20, 21] and also [12]),

$$j_i^{\rm OML} + j_i^{\rm CX} = n_i \sqrt{\frac{k_B T_i}{2\pi m_i}} \left[1 + \frac{Z_p e^2}{R k_B T_i} + 0.1 \frac{\lambda_i^D}{l_{\rm cx}} \left(\frac{Z_p e^2}{R k_B T_i}\right)^2\right] , \tag{20}$$

where $l_{\rm cx} = (\sigma_{\rm cx} n_g)^{-1}$ is the scattering length, $\sigma_{\rm cx}$ is the charge-exchange cross section, and $n_g = p/k_B T_g$ is the gas density.

We start with MF particles confined in a helium discharge. In Fig. 4 we show the power and pressure dependence of the charge of a particle with $R = 4.7\ \mu m$ at rest in the helium discharge of Ref. [33], the plasma parameters of which are given in Table 1. The $p = 102\ Pa$ data point of the $P = 12\ W$ run served as an illustration in Fig. 2. Using the parameters of Table 1 we calculated from Eq. (15) for each data point T_p such that $Z_p(T_p) = Z_{\rm exp}$. The power dependence of the charges, shown in the left panel of Fig. 4, could be reproduced by a single particle temperature $T_p = 405\ K$ while the pressure dependence shown in the right panel required to adjust for each pressure the particle temperature. Assuming T_p to scale with the gas temperature T_g, the predicted particle temperature plotted in the inset of the right panel is in accordance with what we would expect from the pressure dependence of T_g in noble gas discharge [37] indicating that our approach gives physically consistent results. For comparison we also plot the particle charges deduced, respectively, from $j_e^{\rm OML} = j_i^{\rm OML}$ and $j_e^{\rm OML} = j_i^{\rm OML} + j_i^{\rm CX}$. Obviously, the agreement with the data is not very good.

That the charges obtained from the orbital motion limited flux balance are not too close to the experimental data is expected. But even the charge-exchange enhanced flux balance gives not particularly good results. This can be also seen in Fig. 5 where we analyze the charges of MF particles confined in the bulk of the neon discharge of Ref. [12].

The pressure dependence of the charge of a MF particle with $R = 1\ \mu m$ is shown in the left panel of Fig. 5. Since the plasma parameters entering Eq. (15) are known [12], T_p is again the only free parameter. Fixing T_p at a particular value gives the isothermal particle charges $Z_p(T_p)$ shown by the solid lines. From $Z_p(T_p) = Z_{exp}$ follows then the T_p required to reproduce the experimental charge. The predicted increase of T_p with pressure is again in accordance with the results of the calorimetric study of noble gas discharges presented in [37].

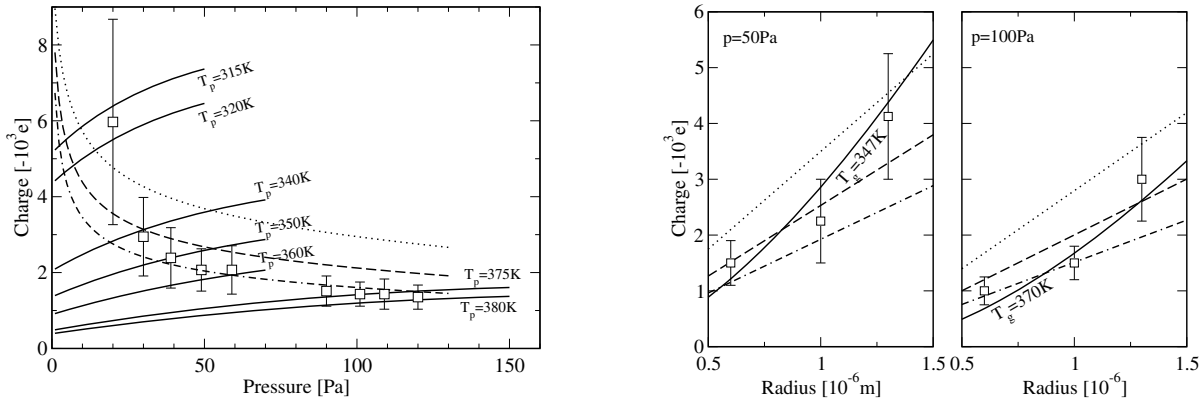

Fig. 5 Left panel: Pressure dependence of the charge of a MF particle with $R = 1\ \mu m$ in the neon discharge of Ref. [12] (squares) [25]. Middle and right panel: Radius dependence of the charge of the MF particle for $p = 50\ Pa$ and $p = 100\ Pa$, respectively. In all panels solid lines denote the (isothermal) charges deduced from the surface model whereas dotted, dashed, and long-dashed lines are the charges obtained from balancing on the grain surface $j_e^{\rm OML}$ with $j_i^{\rm OML} + j_i^{\rm CX}$ using, respectively, $\sigma_{\rm cx} = 0.41 \times 10^{-14} cm^2$ [42], which is the experimentally measured cross section at $0.12\ eV$, $\sigma_{\rm cx} = 1.0 \times 10^{-14} cm^2$, and $\sigma_{\rm cx} = 2.0 \times 10^{-14} cm^2$.

In Fig. 5 we also plot the charges obtained from the charge-exchange enhanced flux balance condition. For $\sigma_{\rm cx} = 2 \times 10^{-14}\ cm^2$ the agreement with the data is in fact quite good but this value of the cross section is almost five times larger than the experimentally measured value ($\sigma_{\rm cx} = 0.41 \times 10^{-14}\ cm^2$ at $0.12\ eV$ [42]). That the agreement with the experimental data is not too good can be also inferred from the radius dependence of Z_p for $p = 50\ Pa$ and $p = 100\ Pa$ which we show, respectively, in the middle and the right panel of Fig. 5.

Clearly, the radius dependence of the grain charge seems to be closer to the nonlinear dependence obtained from Eq. (15) than to the linear dependence resulting from the charge-exchange enhanced flux balance, irrespective of the chosen value of the charge-exchange cross section.

Table 2 Plasma parameters [9] used to obtain the results presented in Fig. 6.

$p[Pa]$	$n_e[10^9 cm^{-3}]$	$kT_e[eV]$	$kT_i[eV]$	$V_{\rm rf}[V]$
6.6	1.7	3.7	0.026	96.4
13.6	2.4	3.9	0.026	96.4

Finally, Fig. 6, showing for two different pressures the radius dependence of Z_p for MF particles confined in the sheath of an argon discharge [10], the plasma parameters of which are given in table 2, provides additional support for our model. To approximately account for the fact that particles with different radius experience different plasma environments, we included the depletion of n_e in the sheath by replacing n_e in $j_e^{\rm OML}$ by $n_e \exp[e\Phi(z_{\rm eq}(R))/k_B T_e]$ with $\Phi(z)$ the sheath potential and $z_{\rm eq}(R)$ the measured equilibrium position of the particle with radius R [10]. When the grains are not too deep in the sheath ($R < 5\ \mu m$), we find for $p = 6.67\ Pa$ and $p = 13.34\ Pa$ excellent agreement with the data for, respectively, $T_p \simeq 410\ K - 430\ K$ and $T_p = 400\ K - 420\ K$, although the particle temperatures are perhaps somewhat too high in view of the small amplitude of the rf voltage. Our approach fails, however, completely for $R > 5\ \mu m$. We attribute this to the ad-hoc modification of the electron flux which may not capture the total electron flux close to the electrode. An improved treatment would calculate the electron flux self-consistently taking not only the depletion of the electron density into account but also the flux due to sub-thermal secondary electrons from the electrode [11].

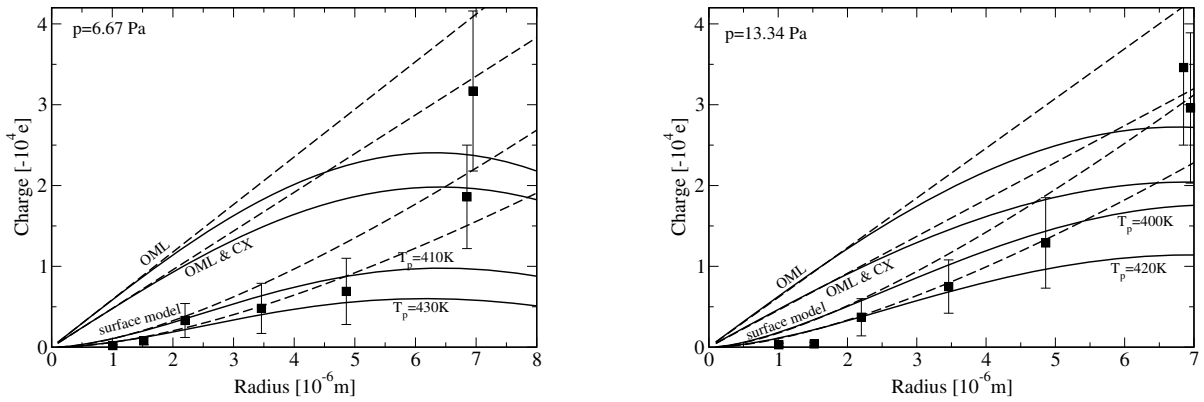

Fig. 6 Radius dependence of the charge of a MF particle in the sheath of an argon discharge at $p = 6.67\ Pa$ (left panel) [25] and $p = 13.34\ Pa$ (right panel). Squares are experimental data from [10] and solid and dashed lines give, respectively, the charges obtained when the depletion of n_e in the confining sheath is included or not. For comparison we also show the charges deduced from $j_e^{\rm OML} = j_i^{\rm OML}$ (OML) and from $j_e^{\rm OML} = j_i^{\rm OML} + j_i^{\rm CX}$ (OML & CX) with $\sigma_{\rm cx} = 0.72 \times 10^{-14} cm^2$ which is the experimentally measured cross section at $0.1\ eV$ [42].

6 Conclusions

In this paper, we discussed the main assumptions underlying the surface model proposed in [25] for the calculation of the charge of a dust particle immersed in a quiescent plasma and confronted the model with additional experimental data.

The main hypothesis of the model, suggested by the analogy of charging of dust particles with physisorption of charged particles to the particles' surface, is that electrons and ions are, on a microscopic scale, spatially separated because the potential in which physisorption of electrons takes place is the attractive short-range polarization potential whereas for ions it is the attractive long-range Coulomb potential. For electrons the analogy may be obvious. But for ions it may be not. However, without the grain no attractive long-range Coulomb potential would exist. Thus, the ion dynamics and kinetics in the vicinity of the grain is also a kind of surface physics although it occurs deep in the disturbed region of the grain and may be strongly affected by the plasma environment.

Within the surface model, the grain charge and its partial screening can be calculated by balancing, on two different surfaces, the electron collection flux with the electron desorption flux and the ion collection flux with

the ion desorption flux. The charge of the grain is then given by the number of electrons quasi-bound in the short-range polarization potential of the grain whereas its partial screening is given by the number of ions quasi-bound in the long-range Coulomb potential.

The grain temperature turns out to be an important parameter. Since, for the experiments we analyzed, the grain temperature has not been measured we used it as an adjustable parameter and obtained for physically meaningful particle temperatures excellent agreement with the experimentally measured grain charges. We challenge therefore experimentalists to simultaneously measure the grain charge and the grain temperature. Our model could then be easily tested.

The charges obtained from the surface model depend on the surface parameter $(s\tau)_e$ which is the product of the electron sticking coefficient with the electron desorption time. Both parameters depend on the inelastic, that is, the dynamic interaction between the electron and the grain. As discussed in [30], a rigorous calculation of $(s\tau)_e$ has to be based on a microscopic model for the electron-grain interaction taking elementary excitations of the grain into account. Quantum-kinetic equations have then to be solved to obtain s_e and τ_e separately. For the product, however, a rough estimate, which turns out to be surprisingly good, can be obtained from the Lennard-Jones-Devonshire formula (13) relating $(s\tau)_e$ to the particle temperature and the electron desorption energy. Measuring these two quantities directly would eliminate any free parameter from our model.

The surface model is a first attempt to treat plasma-controlled electron and ion fluxes and material-controlled plasma-wall interactions at the grain surface on an equal footing. Even in the present rudimentary form the model performs better than approaches relying exclusively on an improvement of the plasma fluxes. Hence, if nothing else, it indicates that the charge a dust particle acquires in a plasma depends not only on the macroscopic plasma environment but also on microscopic processes on the surface occurring on a scale which is beyond the Boltzmann-Poisson description of the plasma-grain interaction. A quantitative theory of grain charging has to be therefore based on a systematic exploration of this ultimate boundary layer.

Acknowledgements Support from the SFB-TR 24 "Fundamentals of Complex Plasmas" is greatly acknowledged. F. X. B. is also grateful to M. Lampe for a particularly illuminating discussion.

References

[1] V.E. Fortov, A.V. Ivlev, S.A. Khrapak, A.G. Khrapak, and G.E. Morfill, Phys. Rep. **421**, 1 (2005).
[2] O. Ishihara, J. Phys. D: Appl. Phys. **40**, R121 (2007).
[3] M. Horányi, Annu. Rev. Astron. Astrophys. **34**, 383 (1996).
[4] I. Mann, Advances in Space Research **41**, 160–167 (2008).
[5] A. Bouchoule (ed.), Dusty Plasmas: Physics, Chemistry, and technological impacts in plasma processing (Wiley and Sons, New York, 1999).
[6] A. Melzer, T. Trottenberg, and A. Piel, Phys. Lett. A **191**, 301 (1994).
[7] T. Trottenberg, A. Melzer, and A. Piel, Plasma Sources Sci. Technol. **4**, 450 (1995).
[8] B. Walch, M. Horányi, and S. Robertson, Phys. Rev. Lett. **75**, 838 (1995).
[9] E.B. Tomme, D.A. Law, B.M. Annaratone, and J.E. Allen, Phys. Rev. Lett. **85**, 2518 (2000).
[10] E.B. Tomme, B.M. Annaratone, and J.E. Allen, Plasma Sources Sci. Technol. **9**, 87 (2000).
[11] A.A. Samarian and S.V. Vladimirov, Phys. Rev. E **67**, 066404 (2003).
[12] S.A. Khrapak, S.V. Ratynskaia, A.V. Zobnin, A.D. Usachev, V.V. Yaroshenko, M.H. Thoma, M. Kretschmer, H. Hoefner, G.E. Morfill, O.F. Petrov, and V. E. Fortov, Phys. Rev. E **72**, 016406 (2005).
[13] I.B. Bernstein and I.N. Rabinowitz, Phys. Fluids **2**, 112 (1959).
[14] J.G. Laframboise and L.W. Parker, Phys. Fluids **16**, 629 (1973).
[15] E.C. Whipple, Rep. Prog. Phys. **44**, 1197 (1981).
[16] J.E. Allen, Phys. Scripta **45**, 497 (1992).
[17] J.E. Daugherty, R.K. Porteous, M.D. Kilgore, and D.B. Graves, J. Appl. Phys. **72**, 3934 (1992).
[18] J.E. Allen, B.M. Annaratone, and U. de Angelis, J. Plasma Phys. **63**, 299 (2000).
[19] R.V. Kennedy and J.E. Allen, J. Plasma Phys. **69**, 485 (2003).
[20] M. Lampe, V. Gavrishchaka, G. Ganguli, and G. Joyce, Phys. Rev. Lett. **86**, 5278 (2001).
[21] M. Lampe, R. Goswami, Z. Sternovsky, S. Robertson, V. Gavrishchaka, G. Ganguli, and G. Joyce, Phys. Plasma **10**, 1500 (2003).
[22] Z. Sternovsky, M. Lampe, and S. Robertson, IEEE Trans. Plasma Science **32**, 632 (2004).
[23] S.A. Khrapak, G.E. Morfill, A.G. Khrapak, and L.G. D'yachkov, Phys. Plasmas **13**, 052114 (2006).
[24] H. Kersten, H. Deutsch, and G.M.W. Kroesen, Int. J. Mass Spectrometry **233**, 51 (2004).

[25] F.X. Bronold, H. Fehske, H. Kersten, and H. Deutsch, Phys. Rev. Lett. **101**, 175002 (2008).
[26] D.D. Tskhakaya, N.L. Tsintsadze, P.K. Shukla, and L. Stenflo, Phys. Scripta **64**, 366 (2001).
[27] D.D. Tskhakaya, P.K. Shukla, and L. Stenflo, Phys. Plasmas **8**, 5333 (2001).
[28] H.J. Kreuzer and Z.W. Gortel, Physisorption Kinetics (Springer Verlag, Berlin, 1986).
[29] W. Brenig and R. Russ, Surface Science **278**, 397 (1992).
[30] F.X. Bronold, H. Fehske, and H. Deutsch, arXiv:0901.4915 (2009).
[31] B.T. Draine and B. Sutin, The Astrophysical Journal **320**, 803 (1987).
[32] C.J.F. Boettcher, Theory of electric polarization (Elsevier Publishing Company, Amsterdam, 1952).
[33] A. Melzer, Der Plasmakristall: Phasenübergang und Stabilität (Verlag Harry Deutsch, Frankfurt am Main, 1997).
[34] M.J. Richardson, Phys. Rev. A **8**, 781 (1973).
[35] V.C. Liu, Space Science Reviews **9**, 423 (1969).
[36] J.E. Lennard-Jones and A.F. Devonshire, Proc. Roy. Soc. (London) A **156**, 6 (1936).
[37] G.H.P.M. Swinkels, H. Kersten, H. Deutsch, and G.M.W. Kroesen, J. Appl. Phys. **88**, 1747 (2000).
[38] H. Helm, J. Phys. B **10**, 3683 (1977).
[39] S. Sinha, S.L. Lin, and J.N. Bardsley, J. Phys. B **12**, 1613 (1979).
[40] S.J. Choi and M.J. Kushner, IEEE Trans. Plasma Science **22**, 138 (1994).
[41] H. Maurer, R. Basner, and H. Kersten, Rev. Sci. Instrum. **79**, 093508 (2008).
[42] R. Hegerberg, M.T. Elford, and H.R. Skullerud, J. Phys. B **15**, 797 (1982).